Macromolecular Rapid Communication
www.mrc-journal.de

Thioacetate-Based Initiators for the Synthesis of Thiol-End-Functionalized Poly(2-oxazoline)s

*Gabriela Gil Alvaradejo, Mathias Glassner, Ravi Kumar, Vanessa Trouillet, Alexander Welle, Yangxin Wang, Victor R. de la Rosa, Sylwia Sekula-Neuner, Michael Hirtz, Richard Hoogenboom, and Guillaume Delaittre**

New functional initiators for the cationic ring-opening polymerization of 2-alkyl-2-oxazolines are described to introduce a thiol moiety at the α terminus. Both tosylate and nosylate initiators carrying a thioacetate group are obtained in multigram scale, from commercial reagents in two steps, including a phototriggered thiol–ene radical addition. The nosylate derivative gives access to a satisfying control over the cationic ring-opening polymerization of 2-ethyl-2-oxazoline, with dispersity values lower than 1.1 during the entire course of the polymerization, until full conversion. Cleavage of the thioacetate end group is rapidly achieved using triazabicyclodecene, thereby leading to a mercapto terminus. The latter gives access to a new subgeneration of α-functional poly(2-oxazoline)s (butyl ester, *N*-hydroxysuccinimidyl ester, furan) by Michael addition with commercial (meth)acrylates. The amenability of the mercapto-poly(2-ethyl-2-oxazoline) for covalent surface patterning onto acrylated surfaces is demonstrated in a microchannel cantilever spotting (μCS) experiment, characterized by X-ray photoelectron spectroscopy (XPS) and time-of-flight secondary-ion mass spectrometry (ToF-SIMS).

Polymer grafting is a powerful method to control surface properties of materials in the biomedical and biotechnological realms, notably with respect to biofouling. Examples include medical implants, biosensors, drug delivery nanovehicles, where interfaces are required to both enhance specific binding and reduce non-specific binding.[1–8] In this context, poly(ethylene glycol) (PEG) has been for a long time considered the gold standard.[9,10] However, due to its degradation mode[11,12] and potential immunogenicity,[13,14] alternative polymers are sought after. Poly(2-alkyl-2-oxazoline)s (PAOx), specifically poly-2-methyl-2-oxazoline (PMeOx) and poly-2-ethyl-2-oxazoline (PEtOx), share some characteristics with PEG, such as stealth behavior, biocompatibility, and low toxicity.[15–17] At the same time, PMeOx and

Dr. G. Gil Alvaradejo, Dr. Y. Wang, Prof. G. Delaittre
Institute of Biological and Chemical Systems (IBCS)
Karlsruhe Institute of Technology (KIT)
Hermann-von-Helmholtz-Platz 1, Eggenstein-Leopoldshafen 76344, Germany

Dr. M. Glassner, Dr. V. R. de la Rosa, Prof. R. Hoogenboom
Supramolecular Chemistry Group
Centre of Macromolecular Chemistry (CMaC)
Department of Organic and Macromolecular Chemistry
Ghent University
Krijgslaan 281-S4, Ghent 9000, Belgium

Dr. R. Kumar, Dr. M. Hirtz
Institute of Nanotechnology (INT)
Karlsruhe Institute of Technology (KIT)
Hermann-von-Helmholtz-Platz 1, Eggenstein-Leopoldshafen 76344, Germany

The ORCID identification number(s) for the author(s) of this article can be found under https://doi.org/10.1002/marc.202000320.

DOI: 10.1002/marc.202000320

V. Trouillet
Institute for Applied Materials (IAM)
Karlsruhe Institute of Technology (KIT)
Hermann-von-Helmholtz-Platz 1, Eggenstein-Leopoldshafen 76344, Germany

Dr. A. Welle
Karlsruhe Institute of Technology (KIT)
Institute of Functional Interfaces
Hermann-von Helmholtz-Platz 1, Eggenstein-Leopoldshafen 76344, Germany

Dr. S. Sekula-Neuner
n.able GmbH
Hermann-von Helmholtz-Platz 1, Eggenstein-Leopoldshafen 76344, Germany

Dr. R. Kumar, V. Trouillet, Dr. A. Welle, Dr. S. Sekula-Neuner, Dr. M. Hirtz
Karlsruhe Institute of Technology (KIT)
Karlsruhe Nano Micro Facility
Hermann-von Helmholtz-Platz 1, Eggenstein-Leopoldshafen 76344, Germany

Prof. G. Delaittre
Organic Functional Molecules
Organic Chemistry
University of Wuppertal
Gaußstrasse 20, Wuppertal 42119, Germany
E-mail: delaittre@uni-wuppertal.de

PEtOx offer the advantage of higher stability, lower viscosity, less demanding synthesis, and large number of functionalization possibilities, notably thanks to functional side chains.[18–20] These features make PAOx promising alternatives for the functionalization of biomaterials.[17,21–23]

The synthesis of PAOx proceeds through cationic ring-opening polymerization (cROP), which allows full control of the polymer properties via tuning of the molar mass distributions and functionality, depending on the choice of the 2-oxazoline monomer(s) and the specific end groups arising from initiation and termination.[19,24–27] Several strategies to graft PAOx on surfaces have been reported.[28,29] A simple and popular method uses α- or ω-functional PAOx prepared with either a functional initiator or a terminating agent, to introduce (directly or after additional modification) a coupling moiety at one chain end.[27] Functionalities introduced by direct end-capping of the living polymer species include trialkoxysilane,[30,31] alkyne,[32] dithiobenzoate,[33] xanthate,[34] methacrylate,[35] methacrylamide,[36] and norbornene,[37] among others, as anchors for the modification of different substrates via the ω end group of PAOx. For this same purpose, functional initiators carrying moieties such as disulfide,[38] allyl,[30] alkyne,[39] or coumarin,[40] to name but a few, were used to produce α-functionalized PAOx.

Here, we present a strategy for the synthesis of well-defined functional α-thiolated PAOx. Thiols are popular reactive groups because of their ability to engage in a wide range of reactions with compounds such as halides,[41] pentafluorophenylalkanes,[42] alkenes,[43] alkynes,[44] disulfides.[45] In the context of end-functional PAOx, thiol moieties have exclusively been introduced at the ω chain end, where it was introduced by direct termination with sodium hydrosulfide[46] or by postmodification of ω end groups such as xanthate[44,46] or diallylamino.[47] To the best of our knowledge, a thiol group was never introduced at the α position of PAOx chains. In the present contribution, we report the synthesis and characterization of two initiators for the cROP of 2-oxazolines and introduction of a masked thiol functionality at the α chain end. After deprotection, we demonstrate the reactivity of the thiol end group using various alkenes, enabling the introduction of alternative functionality to the α terminus. Finally, we show that the as-synthesized α-mercapto PEtOx is amenable to highly localized grafting onto acrylated substrates using a fine surface patterning method, i.e., microchannel cantilever spotting (μCS).[48–51]

Since the thiol moiety is an excellent nucleophile, it may interfere with the cROP process. A classic method to circumvent such issues in organic and polymer chemistry is the recourse to protecting groups. This method has been rather parsimoniously used in the synthesis of α-functional PAOx. Example of protecting groups incorporated in cROP initiators include *N*-alkylphthalimide or *tert*-butyl *N*-monoalkylcarbamate (for amines),[52–56] *tert*-butyldiphenylsilyl ethers (for hydroxyl),[57] methyl ester (for carboxylic acid or others through amidation),[58–63] and furanyl Diels–Alder cycloadduct (for maleimide).[64] Here, the thioacetate group has been chosen as a stable and economic protection group for thiols.[65] In the case of the tosylate initiator, **ThioAcTos** (**Scheme 1**), the synthetic route started with the nucleophilic substitution of allyl alcohol with tosyl chloride to yield allyl tosylate **1** (Scheme S1, Supporting Information). The corresponding initiator **ThioAcTos**

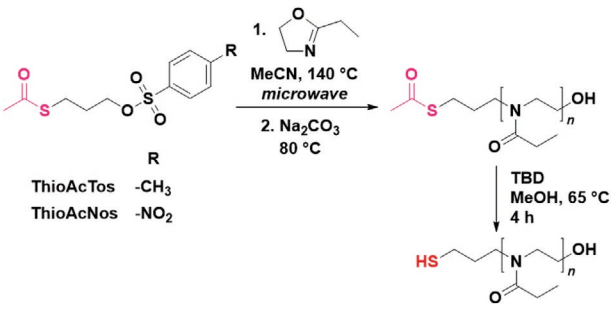

Scheme 1. Synthetic route for the synthesis of α-thiolated PEtOx by polymerization of EtOx using functional initiators **ThioAcTos** and **ThioAcNos** and base-triggered deprotection.

was obtained by phototriggered thiol–ene radical addition of **1** with thioacetic acid. An alternative route for the synthesis of the nosylate initiator (**ThioAcNos**) was designed, because purification of the products obtained following the previous strategy proved to be a more challenging task. **ThioAcNos** was obtained after nosylation of the product of the thiol–ene addition between thioacetic acid and allyl alcohol (**2**). This led to a more straightforward purification avoiding chromatographic steps and resulting in higher yields. Analysis of both initiators by ^{1}H and ^{13}C NMR spectroscopy, as well as electrospray ionization mass spectrometry (ESI-MS), confirmed that the targeted structures were obtained with high purity (Figures S1–S6, Supporting Information).

The polymerization was performed using optimized microwave conditions,[66] at 140 °C and with acetonitrile as reaction solvent (Scheme 1). To assess the ability of both initiators to start the polymerization, a first set of experiments was carried out for 7.5 minutes with [EtOx] = 4 M and [EtOx]/[initiator] = 50. Full conversion was achieved in both cases; however, the corresponding size-exclusion chromatography (SEC) traces revealed distinct dispersity values of 1.20 and 1.10 for **ThioAcTos** and **ThioAcNos**, respectively (Figure S7, Supporting Information). The broader molar mass distribution obtained when initiating the polymerization with **ThioAcTos** may be the result of a lower electrophilicity of this initiator, leading to a lower initiation rate.[67] It is nevertheless conceivable that **ThioAcTos** is a suitable initiator for the polymerization of more nucleophilic monomers such as MeOx. However, we did not investigate this further and concentrated on **ThioAcNos** because it will offer more versatility in terms of accessible 2-alkyl-2-oxazoline monomers. The living character of the polymerization was successfully shown via kinetic studies using three different monomer-to-initiator ratios (20, 40, and 60) (**Figure 1**). As expected, the polymerization proceeds faster when a lower [EtOx]/[**ThioAcNos**] ratio is used (Figure 1A).[68] All kinetics showed a linear behavior, indicating a constant concentration of the propagating species. The apparent k_p values are rather similar (Table S1, Supporting Information) and therefore appear to be independent of the initial monomer-to-initiator concentration, as reported in previous studies.[68] Additionally, SEC analysis of the samples taken at various time intervals evidenced a linear increase of the number-average molar masses (M_n) and dispersity values consistently below 1.1 (Figure 1B). A clear uniform shift towards higher retention times can be

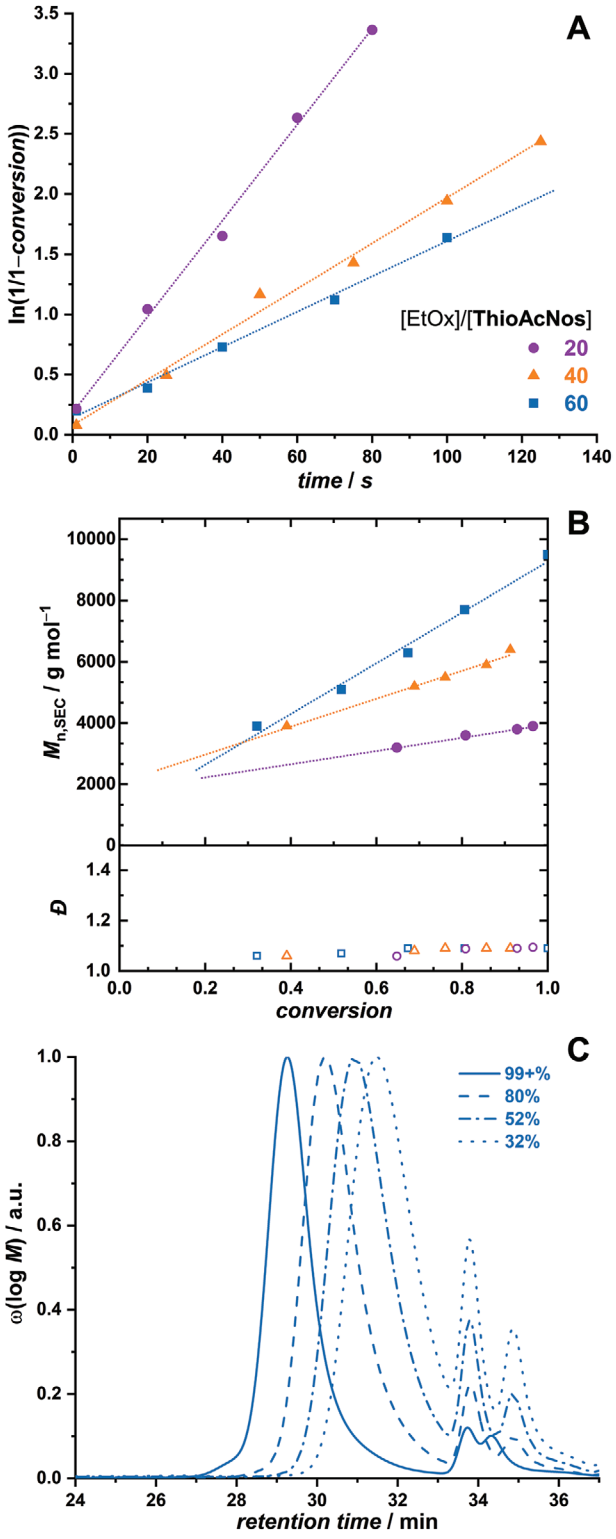

Figure 1. A) First-order kinetic plots and B) evolution of the number-average molar mass and dispersity with conversion for the cROP of EtOx initiated by **ThioAcNos** in MeCN at 140 °C at [EtOx] = 4 M and various [EtOx]/[**ThioAcNos**]. All dotted lines correspond to linear fits with r^2 = 0.99. C) Size-exclusion chromatograms corresponding to the series with [EtOx]/[**ThioAcNos**] = 60.

observed (Figure 1C; Figure S8, Supporting Information). The discrepancy between theoretical and experimental M_n values comes from the fact that the latter are calculated relative to poly(methyl methacrylate) standards, which results in an overestimation of the molar mass.[69]

A purified polymer, **ThioAc-PEtOx**, obtained with [EtOx]/[**ThioAcNos**] = 40, was used to confirm the nature of the end groups, and for further deprotection and modification. In NMR spectra, although the acetate methyl group signal overlaps with those corresponding to the PEtOx side-chain methylene groups, signals of all methylene protons located between the sulfur atom and the first nitrogen atom of the polymer chain appear independently and confirm the presence of the end group (Figure S9, Supporting Information). These methylene proton signals could also be used to calculate the degree of polymerization of the **ThioAc-PEtOx** and provided values closer to the expected ones than SEC (see Table S2 in the Supporting Information). ESI-MS also confirmed the structure of the polymer (**Figure 2**, black spectrum). Note that double-charged species are represented here. The main population was assigned to the thioacetate-functionalized PEtOx chains with an ω hydroxyl end group arising from termination with sodium carbonate. Besides, a population was observed arising from proton-initiation, either due to residual protic sources (e.g., water) or β-termination.[24] Two further minor populations were also detected, yet not assigned. It is however noteworthy that these vanish during subsequent steps, which suggests they correspond to chains carrying the thioacetate moiety.

Deprotection was initially attempted using sodium hydroxide and tetramethylammonium hydroxide, yet without any success (broad distributions). Eventually, triazabicyclodecene (TBD), a strong yet selective guanidine base, led to full deprotection and yielded **Thio-PEtOx**, as evidenced via ESI-MS measurement by the negative shift of 21 amu (i.e., 42/2), corresponding to the loss of the acetate group (Figure 2, red spectrum). The analysis by SEC revealed more challenging. Indeed, the as-deprotected product led to a multimodal distribution, clearly indicating the presence of a population with molar masses similar to those of the parent **ThioAcPEtOx**, as well as a main distribution with approximately twice the molar mass (**Figure 3**, dotted red line). This can clearly be attributed to disulfide coupling. Incubating the deprotected polymer solution with a reducing agent such as dithiothreitol (DTT) did reduce the occurrence of coupled chains but did not fully suppress it (Figure 3, full red line).

As previously mentioned, the versatility of the thiol group allows a wide range of reactions. In this study, we first wanted to briefly showcase that **Thio-PEtOx** could be used as an access point to further α-functional PEtOx, particularly making use of the large variety of commercial functional Michael acceptors, such as acrylates and methacrylates. Conditions chosen for the base-catalyzed thiol–ene addition are depicted in Figure 2 (top): with dimethylphenylphosphine (DMPP) playing the dual role of reducing agent and base, in acetone at ambient temperature. The first reaction was performed with *n*-butyl acrylate (BA), leading to a slightly amphiphilic structure. ESI-MS measurement evidenced a shift of the main population corresponding to the addition of the acrylate (Figure 2, blue spectrum). Importantly,

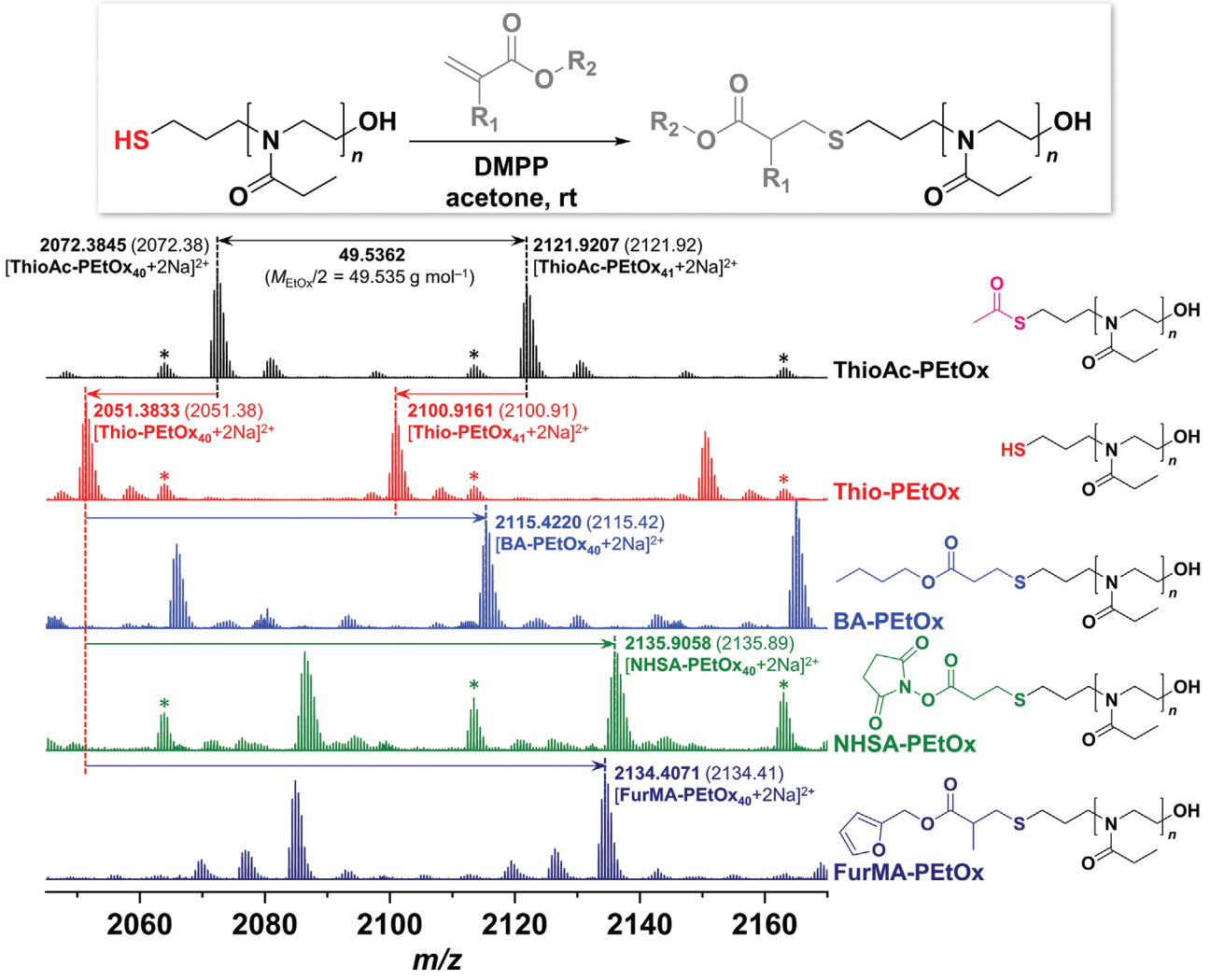

Figure 2. (Top) DMPP-catalyzed Michael addition of (meth)acrylics onto **ThioPEtOx**. (Bottom) ESI-MS spectra of A) **ThioAc-PEtOx** as obtained after cROP of EtOx initiated by **ThioAcNos**, B) **Thio-PEtOx** obtained after treatment with TBD of **ThioAc-PEtOx**, C) the Michael addition product of **Thio-PEtOx** with butylacrylate (**BA-PEtOx**), D) acrylic acid *N*-hydroxysuccinimide ester (**NHSA-PEtOx**), and E) furfuryl methacrylate (**FurMA-PEtOx**). H-initiated, non α-functional chains are marked with an asterisk.

the SEC trace of **BA-PEtOx** displayed a near-monomodal distribution (Figure 3, blue line), which closely reproduced the distribution of the protected **ThioAc-PEtOx**, demonstrating a clean deprotection–functionalization sequence and confirming the origin of the second population observed for **Thio-PEtOx**.

In order to showcase the versatility of the new **Thio-PEtOx** as an entry point for further end-functional poly(2-oxazoline)s, we then performed a similar end-group modification with two (meth)acrylates that carry a reactive group in the ester side chain, namely acrylic acid *N*-hydroxysuccinimide ester (NHSA) and furfuryl methacrylate (FurMA). The respective products, **NHSA-PEtOx** and **FurMA-PEtOx**, were detected as main species in ESI-MS (Figure 2, green and dark blue spectra, respectively). SEC characterization indicated a similar outcome as for the functionalization with BA (Figure S10, Supporting Information). For NHSA, however, a secondary distribution with approximately a doubled molar mass is visible. It could arise from undesired reaction of the NHS ester with thiol end groups, leading to covalently coupled chains, as some succinimidyl ester have been found to react with cysteine side chains for instance.[70] Yet, no vinyl signals were observed in ^{1}H NMR spectrum (not shown). It is therefore assumed that the present reaction did not go to completion.

We further aimed at demonstrating the possibility to pattern thiolated PEtOx onto flat surfaces by Michael addition. Indeed, PEtOx has been involved in several studies related to biointerfaces, particularly to control bioadhesion.[21,22,28,29] In the present case, we harnessed microchannel cantilever spotting (μCS)[48–51] to position microdroplets of a reactive PEtOx ink onto a functionalized surface, here an acrylated Si wafer (**Figure 4**A). The droplets then act as microreactors in which covalent grafting to the surface occurs. The ink consisted of **Thio-PEtOx**, DMPP and glycerol—to tune viscosity and evaporation—in DMSO. A control ink in which **Thio-PEtOx** was replaced with a non-functional PEtOx was also spotted. All samples were thoroughly washed after reaction. Figure 4B depicts the droplet pattern imaged by optical microscopy, directly after the μCS step: Dots

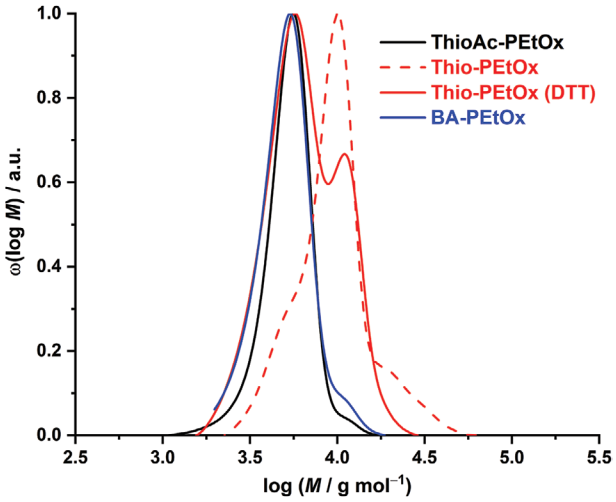

Figure 3. Overlay of SEC traces of **ThioAc-PEtOx** ($M_{n,SEC}$ = 6500 g mol^{-1}, $Đ$ = 1.20; $M_{n,NMR}$ = 4400 g mol^{-1}), its deprotection product **Thio-PEtOx** with and without a reducing agent (DTT), and **BA-PEtOx** obtained by Michael addition of **Thio-PEtOx** with *n*-butyl methacrylate.

with a diameter of ≈15 µm were arranged with a 30 µm spacing. X-ray photoelectron spectroscopy (XPS) analysis of the activated wafer showed a total carbon content of 4.3 at% at the surface, attributed to contaminants (Figure 4C bottom and Table S2 in the Supporting Information). After functionalization with 3-(trimethoxysilyl)propyl acrylate, the total carbon content increased significantly to 19.7 at% and the appearance of a peak at 289.2 eV was observed (Figure 4C middle), proving the presence of the O—C=O species of the acrylic polysiloxane layer with a contribution of 3.5 at%. After **Thio-PEtOx** patterning, an intensity decrease of this latter signal (1.1 at%) indicated successful surface modification (Figure 4C bottom). Concomitantly, the appearance of an additional peak at 288.4 eV, attributed to amide groups,[71] was observed with a concentration of 0.5 at% (Figure 4C top), proving functionalization with PEtOx. Also, the corresponding signal at 400.1 eV (0.5 at%) indicates the presence of nitrogen atoms on the surface with a 1:1 ratio to the amide carbon (Table S2, Supporting Information). Finally, time-of-flight secondary-ion mass spectrometry (ToF-SIMS), which offers a greater spatial resolution and can therefore independently probe the spotted areas and their surroundings, confirmed the presence of chemical patterns: Dots rich in CN,

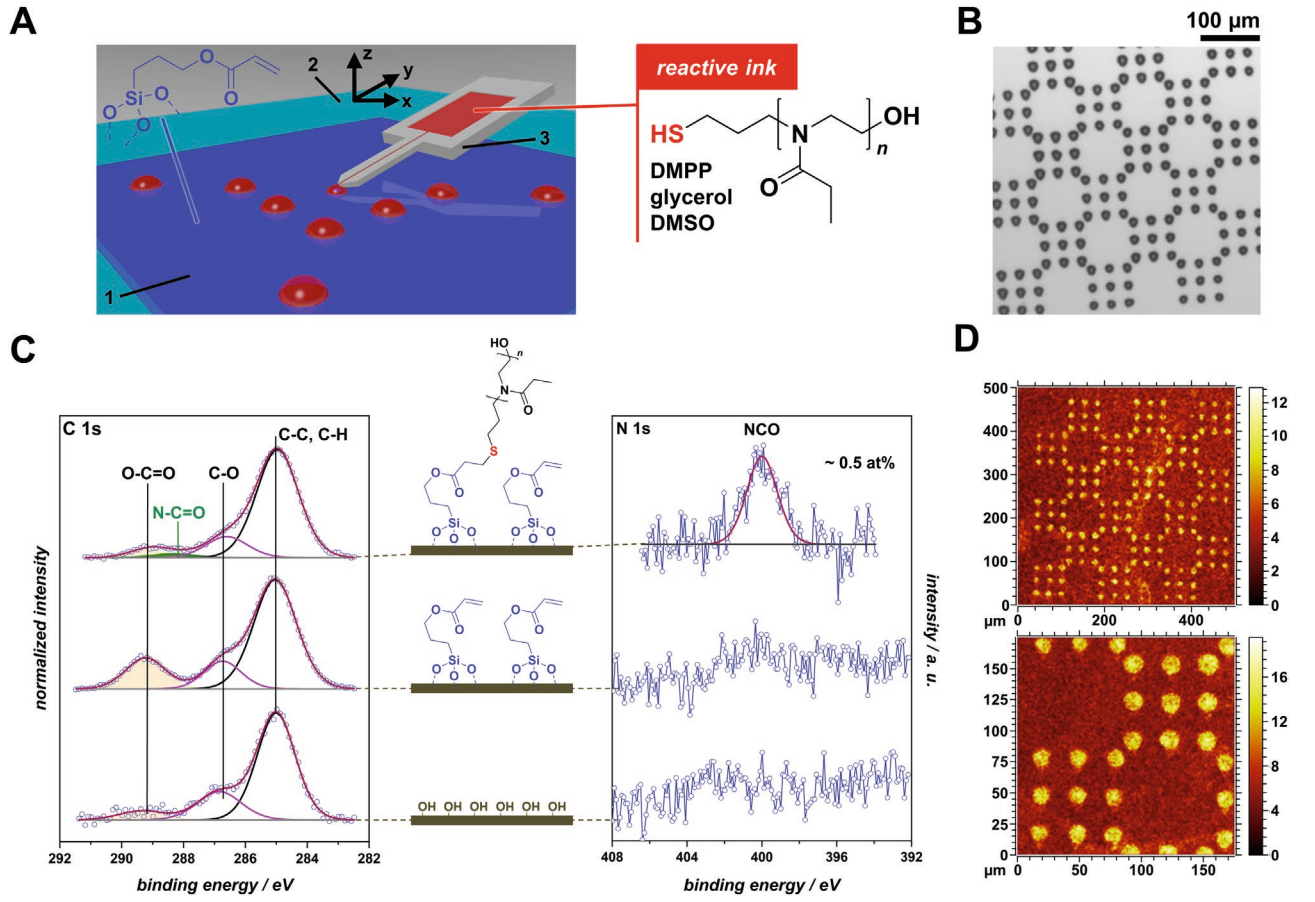

Figure 4. A) Schematic representation of the patterning of **Thio-PEtOx** onto an acrylated surface using µCS. The acrylated Si wafer (1) is placed on the stage (2), which can be actuated with a precision of less than 100 nm in the *x*, *y*, and *z* directions by piezoelectric actuators. By raising the stage in the *z* direction, the substrate can be brought into contact with the apex of the microchannel cantilever (3) on which the polymer solution reservoir is located. B) Optical image showing the ink pattern formed after the µCS step. C) C 1s and N 1s XPS spectra of the Si wafer before and after modifications. D) ToF-SIMS chemical mapping (sum of CN^-, CNO^-, S^-, and HS^- fragments) of the patterned acrylated silicon wafer.

CNO, S, and SH species on a background poor in these species are clearly identified (Figure 4D top; Figures S11 and S12, Supporting Information). The pattern fidelity, with respect to the initial droplet array, is very high (Figure 4D bottom; Figure S13, Supporting Information). Importantly, the control ink did not show any pattern, thereby demonstrating that **ThioPEtOx** covalently reacted with the surface, and did not just adsorb.

In the present contribution, we reported two new thioacetate-functionalized initiators for the cationic polymerization of 2-alkyl-2-oxazolines. The nosylate version revealed to be most suitable for the polymerization of 2-ethyl-2-oxazoline in acetonitrile, achieving near-quantitative conversion, low dispersity, and full α end-group retention, within minutes at 140 °C under microwave irradiation. Full deprotection could be performed using an organic guanidine base, namely triazabicyclodecene. Precise characterization of the polymer with a free thiol α end group proved challenging due to the occurrence of disulfide coupling. Nevertheless, further functionalization by Michael addition with functional (meth)acrylates unambiguously confirmed a clean transformation. It is incidentally demonstrated that the α-mercapto poly(2-ethyl-2-oxazoline) is an access point to generations of α-functional polymers by virtue of the large range of available and accessible (meth)acrylic derivatives, themselves being further potential access points, in the present case by further amidation or Diels–Alder cycloaddition.

Finally, the α-mercapto poly(2-ethyl-2-oxazoline) was successfully patterned in a covalent way onto acrylated surfaces using a soft micro/nanolithography method, namely microchannel cantilever spotting. This appears promising for the design of micro/nanostructured biointerfaces, in which poly(2-ethyl-2-oxazoline) could act as antibioadhesive barrier. Further methods of patterned immobilization, such as photoinitiated thiol–ene addition could be envisaged as well.

Supporting Information

Supporting Information is available from the Wiley Online Library or from the author.

Acknowledgements

G.G.A. thanks the Mexican National Council for Science and Technology (Conacyt) for a doctoral research scholarship. Y.W. thanks the China Scholarship Council for financial support (No. 201806295022). This work was partly carried out with the support of the Karlsruhe Nano Micro Facility (KNMF, www.knmf.kit.edu), a Helmholtz Research Infrastructure at Karlsruhe Institute of Technology (KIT, www.kit.edu).

Open access funding enabled and organized by Projekt DEAL.

Conflict of Interest

The authors declare no conflict of interest.

Keywords

protecting groups, ring-opening polymerization, surface patterning, telechelic, thiol–ene

Received: June 14, 2020
Revised: July 14, 2020
Published online: August 16, 2020

[1] I. Banerjee, R. C. Pangule, R. S. Kane, *Adv. Mater.* **2011**, *23*, 690.
[2] A. Hucknall, S. Rangarajan, A. Chilkoti, *Adv. Mater.* **2009**, *21*, 2441.
[3] J. E. Raynor, J. R. Capadona, D. M. Collard, T. A. Petrie, A. J. García, *Biointerphases* **2009**, *4*, FA3.
[4] W. Senaratne, L. Andruzzi, C. K. Ober, *Biomacromolecules* **2005**, *6*, 2427.
[5] D. Campoccia, L. Montanaro, C. R. Arciola, *Biomaterials* **2013**, *34*, 8533.
[6] K. Yu, Y. Mei, N. Hadjesfandiari, J. N. Kizhakkedathu, *Colloids Surf., B* **2014**, *124*, 69.
[7] M. A. Rufin, M. A. Grunlan, in *Funct. Polym. Coatings* (Eds: L. Wu, J. Baghdachi), John Wiley & Sons, Inc, Hoboken, NJ **2015**, pp. 218–238.
[8] M. Badoux, M. Billing, H. A. Klok, *Polym. Chem.* **2019**, *10*, 2925.
[9] J. H. Lee, H. B. Lee, J. D. Andrade, *Prog. Polym. Sci.* **1995**, *20*, 1043.
[10] A. Kolate, D. Baradia, S. Patil, I. Vhora, G. Kore, A. Misra, *J. Controlled Release* **2014**, *192*, 67.
[11] B. Pidhatika, M. Rodenstein, Y. Chen, E. Rakhmatullina, A. Muehlebach, C. Acikgoz, M. Textor, R. Konradi, *Biointerphases* **2012**, *7*, 1.
[12] J. Ulbricht, R. Jordan, R. Luxenhofer, *Biomaterials* **2014**, *35*, 4848.
[13] R. P. Garay, R. El-Gewely, J. K. Armstrong, G. Garratty, P. Richette, *Expert Opin. Drug Delivery* **2012**, *9*, 1319.
[14] H. Schellekens, W. E. Hennink, V. Brinks, *Pharm. Res.* **2013**, *30*, 1729.
[15] T. X. Viegas, M. D. Bentley, J. M. Harris, Z. Fang, K. Yoon, B. Dizman, R. Weimer, A. Mero, G. Pasut, F. M. Veronese, *Bioconjug. Chem.* **2011**, *22*, 976.
[16] R. Hoogenboom, *Angew. Chem., Int. Ed.* **2009**, *48*, 7978.
[17] N. Adams, U. S. Schubert, *Adv. Drug Delivery Rev.* **2007**, *59*, 1504.
[18] B. Guillerm, V. Darcos, V. Lapinte, S. Monge, J. Coudane, J.-J. Robin, *Chem. Commun.* **2012**, *48*, 2879.
[19] K. Lava, B. Verbraeken, R. Hoogenboom, *Eur. Polym. J.* **2015**, *65*, 98.
[20] M. A. Mees, R. Hoogenboom, *Polym. Chem.* **2018**, *9*, 4968.
[21] M. Bauer, C. Lautenschlaeger, K. Kempe, L. Tauhardt, U. S. Schubert, D. Fischer, *Macromol. Biosci.* **2012**, *12*, 986.
[22] R. Konradi, C. Acikgoz, M. Textor, *Macromol. Rapid Commun.* **2012**, *33*, 1663.
[23] V. R. De La Rosa, *J. Mater. Sci.: Mater. Med.* **2014**, *25*, 1211.
[24] B. Verbraeken, B. D. Monnery, K. Lava, R. Hoogenboom, *Eur. Polym. J.* **2017**, *88*, 451.
[25] M. Glassner, M. Vergaelen, R. Hoogenboom, *Polym. Int.* **2018**, *67*, 32.
[26] G. Gil Alvaradejo, M. Glassner, R. Hoogenboom, G. Delaittre, *RSC Adv.* **2018**, *8*, 9471.
[27] G. Delaittre, *Eur. Polym. J.* **2019**, *121*, 109281.
[28] G. Morgese, E. M. Benetti, *Eur. Polym. J.* **2017**, *88*, 470.
[29] L. Tauhardt, K. Kempe, M. Gottschaldt, U. S. Schubert, *Chem. Soc. Rev.* **2013**, *42*, 7998.
[30] Y. Chujo, E. Ihara, S. Kure, T. Saegusa, *Macromolecules* **1993**, *26*, 5681.
[31] T. Li, C. Zhou, M. Jiang, *Polym. Bull.* **1991**, *25*, 211.
[32] E. D. H. Mansfield, K. Sillence, P. Hole, A. C. Williams, V. V. Khutoryanskiy, *Nanoscale* **2015**, *7*, 13671.
[33] D. Le, F. Wagner, M. Takamiya, I.-L. Hsiao, G. Gil Alvaradejo, U. Strähle, C. Weiss, G. Delaittre, *Chem. Commun.* **2019**, *55*, 3741.
[34] V. R. de la Rosa, Z. Zhang, B. G. De Geest, R. Hoogenboom, *Adv. Funct. Mater.* **2015**, *25*, 2511.

[35] I. Yildirim, T. Bus, M. Sahn, T. Yildirim, D. Kalden, S. Hoeppener, A. Traeger, M. Westerhausen, C. Weber, U. S. Schubert, *Polym. Chem.* **2016**, *7*, 6064.
[36] C. P. Fik, S. Konieczny, D. H. Pashley, C. J. Waschinski, R. S. Ladisch, U. Salz, T. Bock, J. C. Tiller, *Macromol. Biosci.* **2014**, *14*, 1569.
[37] G. G. Alvaradejo, H. V. T. Nguyen, P. Harvey, N. M. Gallagher, D. Le, M. F. Ottaviani, A. Jasanoff, G. Delaittre, J. A. Johnson, *ACS Macro Lett.* **2019**, *8*, 473.
[38] T. Lehmann, J. Rühe, *Macromol. Symp.* **1999**, *142*, 1.
[39] C. Haensch, T. Erdmenger, M. W. M. Fijten, S. Hoeppener, U. S. Schubert, *Langmuir* **2009**, *25*, 8019.
[40] L. Korchia, C. Bouilhac, V. Lapinte, C. Travelet, R. Borsali, J. J. Robin, *Polym. Chem.* **2015**, *6*, 6029.
[41] Y. Zhang, G. Chen, Y. Lin, L. Zhao, W. Z. Yuan, P. Lu, C. K. W. Jim, Y. Zhang, B. Z. Tang, *Polym. Chem.* **2015**, *6*, 97.
[42] G. Delaittre, L. Barner, *Polym. Chem.* **2018**, *9*, 2679.
[43] H. Turgut, G. Delaittre, *Chem. – Eur. J.* **2016**, *22*, 1511.
[44] M. Hartlieb, T. Floyd, A. B. Cook, C. Sanchez-Cano, S. Catrouillet, J. A. Burns, S. Perrier, *Polym. Chem.* **2017**, *8*, 2041.
[45] O. Schäfer, M. Barz, *Chem. – Eur. J.* **2018**, *24*, 12131.
[46] Y. Shimano, K. Sato, S. Kobayashi, *J. Polym. Sci., Part A: Polym. Chem.* **1995**, *33*, 2715.
[47] O. Koshkina, T. Lang, R. Thiermann, D. Docter, R. H. Stauber, C. Secker, H. Schlaad, S. Weidner, B. Mohr, M. Maskos, A. Bertin, *Langmuir* **2015**, *31*, 8873.
[48] J. Xu, M. Lynch, J. L. Huff, C. Mosher, S. Vengasandra, G. Ding, E. Henderson, *Biomed. Microdevices* **2004**, *6*, 117.
[49] M. Hirtz, A. M. Greiner, T. Landmann, M. Bastmeyer, H. Fuchs, *Adv. Mater. Interfaces* **2014**, *1*, 1300129.
[50] S. M. M. Dadfar, S. Sekula-Neuner, U. Bog, V. Trouillet, M. Hirtz, *Small* **2018**, *14*, 1800131.
[51] J. Atwater, D. S. Mattes, B. Streit, C. von Bojničić-Kninski, F. F. Loeffler, F. Breitling, H. Fuchs, M. Hirtz, *Adv. Mater.* **2018**, *30*, 1801632.
[52] R. Obeid, C. Scholz, *Biomacromolecules* **2011**, *12*, 3797.
[53] D. Witzigmann, D. Wu, S. H. Schenk, V. Balasubramanian, W. Meier, J. Huwyler, *ACS Appl. Mater. Interfaces* **2015**, *7*, 10446.
[54] L. Y. Qiu, L. Yan, L. Zhang, Y. M. Jin, Q. H. Zhao, *Int. J. Pharm.* **2013**, *456*, 315.
[55] C. J. Waschinski, J. C. Tiller, *Biomacromolecules* **2005**, *6*, 235.
[56] M. J. Isaacman, W. Cui, L. S. Theogarajan, *J. Polym. Sci., Part A: Polym. Chem.* **2014**, *52*, 3134.
[57] M. Reif, R. Jordan, *Macromol. Chem. Phys.* **2011**, *212*, 1815.
[58] S. Zalipsky, C. B. Hansen, J. M. Oaks, T. M. Allen, *J. Pharm. Sci.* **1996**, *85*, 133.
[59] Y. Chen, W. Cao, J. Zhou, B. Pidhatika, B. Xiong, L. Huang, Q. Tian, Y. Shu, W. Wen, I. M. Hsing, H. Wu, *ACS Appl. Mater. Interfaces* **2015**, *7*, 2919.
[60] Y. Gao, Y. Li, Y. Li, L. Yuan, Y. Zhou, J. Li, L. Zhao, C. Zhang, X. Li, Y. Liu, *Nanoscale* **2015**, *7*, 597.
[61] J. Li, Y. Zhou, C. Li, D. Wang, Y. Gao, C. Zhang, L. Zhao, Y. Li, Y. Liu, X. Li, *Bioconjug. Chem.* **2015**, *26*, 110.
[62] Y. Chen, C. Yang, J. Mao, H. Li, J. Ding, W. Zhou, *RSC Adv.* **2019**, *9*, 11026.
[63] A. Podevyn, K. Arys, V. R. de la Rosa, M. Glassner, R. Hoogenboom, *Eur. Polym. J.* **2019**, *120*, 109273.
[64] G. Gil Alvaradejo, M. Glassner, R. Hoogenboom, G. Delaittre, *RSC Adv.* **2018**, *8*, 9471.
[65] F. Goethals, D. Frank, F. Du Prez, *Prog. Polym. Sci.* **2017**, *64*, 76.
[66] F. Wiesbrock, R. Hoogenboom, M. A. M. Leenen, M. A. R. Meier, U. S. Schubert, *Macromolecules* **2005**, *38*, 5025.
[67] M. Glassner, D. R. D'Hooge, J. Y. Park, P. H. M. Van Steenberge, B. D. Monnery, M.-F. Reyniers, R. Hoogenboom, *Eur. Polym. J.* **2015**, *65*, 298.
[68] R. Hoogenboom, M. W. M. Fijten, U. S. Schubert, *J. Polym. Sci., Part A: Polym. Chem.* **2004**, *42*, 1830.
[69] P. J. M. Bouten, D. Hertsen, M. Vergaelen, B. D. Monnery, M. A. Boerman, H. Goossens, S. Catak, J. C. M. Van Hest, V. Van Speybroeck, R. Hoogenboom, *Polym. Chem.* **2015**, *6*, 514.
[70] S. Abad, P. Nolis, J. D. Gispert, J. Spengler, F. Albericio, S. Rojas, J. R. Herance, *Chem. Commun.* **2012**, *48*, 6118.
[71] K. Rück-Braun, M. Å. Petersen, F. Michalik, A. Hebert, D. Przyrembel, C. Weber, S. A. Ahmed, S. Kowarik, M. Weinelt, *Langmuir* **2013**, *29*, 11758.